International Journal of Impact Engineering 125 (2019) 163–172

Contents lists available at ScienceDirect

International Journal of Impact Engineering

journal homepage: www.elsevier.com/locate/ijimpeng

Crushing resistance and energy absorption of pomelo peel inspired hierarchical honeycomb

Zhang Wen[a,b,c], Yin Sha[a,b], Yu T.X.[d], Xu Jun[a,b,*]

[a] Department of Automotive Engineering, School of Transportation Science and Engineering, Beihang University, Beijing 100191, China
[b] Advanced Vehicle Research Center (AVRC), Beihang University, Beijing 100191, China
[c] Shenyuan Honors College, Beihang University, Beijing 100191, China
[d] Department of Mechanical & Aerospace Engineering, The Hong Kong University of Science and Technology, Clear Water Bay, Kowloon, Hong Kong

ARTICLE INFO

Keywords:
Bio-inspired honeycomb
Structural hierarchy
Crushing resistance
Energy absorption

ABSTRACT

Hierarchical materials born of variable natural cellular and intricate architecture are demonstrated to have the potential to achieve outstanding mechanical properties, thus make them excellent constituents for impact protection. Inspired by the unique microstructure of pomelo peel, this study constructed a novel hierarchical honeycomb and investigated the crushing resistance along with energy absorption capabilities of such structural materials. An integrated analytical-numerical approach was developed to fully elucidate the underlying quantitative structure-property relations by parametric studies on the evaluation of different hierarchical orders and equivalent thickness. It is revealed that the deformation modes of pomelo peel inspired honeycomb are governed by the geometric parameter-equivalent thickness, where three deformation modes (hexagonal mode, transitional mode and coin mode) and two localized band ("V" mode and "I" mode) can be observed under out-of-plane and in-plane crushing, respectively. Additionally, in conjunction with theoretical and numerical studies, improved crushing resistance and energy absorption properties of the pomelo peel inspired honeycomb can be obtained via increase of structural hierarchy and variation of geometric dimensions. The crushing resistance criteria, *SEA* (specific energy absorption) and equivalent plateau stress of hierarchical honeycomb, can be enhanced up to 1.5 and 2.5 times than its counterpart for traditional honeycomb under out-of-plane and in-plane crushing, respectively. The promising results of pomelo peel inspired honeycomb may exhibit a novel perspective on providing the superior mechanical properties of natural cellular materials and offer insights for applications of bio-inspired engineering materials.

1. Introduction

Natural materials always offer novel insights into exploring, designing, synthesizing and fabricating advanced materials with superior mechanical performance (e.g., high energy absorption [1–4], low density and high specific strength [5]) using limited continuous basic material, especially cellular materials (e.g., wood and bone [6,7]). More recently, researchers continue to be fascinated by novel natural materials with hierarchical or gradient structures, which largely contributes toward customized mechanical properties for artificial materials used in engineering applications [8–12].

Mature pomelos (*Citrus maxima*), weighing up to 6 kg [13] and growing on trees with heights of up to 15 m [14], have considerable kinetic energy to be absorbed as they fall to the ground, leading to the inevitable consideration of impact protection. In addition, given the fact that animals are the main dispersal vectors of pomelo seeds, severe damage of pomelo during impact on the ground may give rise to intensifying competition among animals and microbes (like fungi and bacteria), decreasing the germination capacity of pomelo [15]. Hence, pomelo peel, known as natural protecting barrier for pulp and seed inside, has been identified to be capable of energy dissipation on account of the porous hierarchical structure through experimental studies [15–18]. Fischer et al. demonstrated good impact resistance of pomelo peel via freefall tests of whole pomelos [16]. It has been also proved through experiments that the decomposition of fruits by microbes would greatly block Citrus seed dispersal if the pomelo peel split open due to the impact on the ground [15]. As depicted in Fig. 1, the thickness of pomelo peel is typically 2–3 cm, consisting of flavedo (exocarp) and albedo (spongy mesocarp, main part of the peel), where dense vascular bundles surrounded by loose biological tissues can be observed by scanning electron microscope (SEM). Researches on the influence of governing factors (e.g., the hydration state [19], density

* Corresponding author at: Department of Automotive Engineering, School of Transportation Science and Engineering, Beihang University, Beijing 100191, China.
E-mail address: junxu@buaa.edu.cn (J. Xu).

https://doi.org/10.1016/j.ijimpeng.2018.11.014
Received 25 June 2018; Received in revised form 22 November 2018; Accepted 25 November 2018
Available online 26 November 2018
0734-743X/

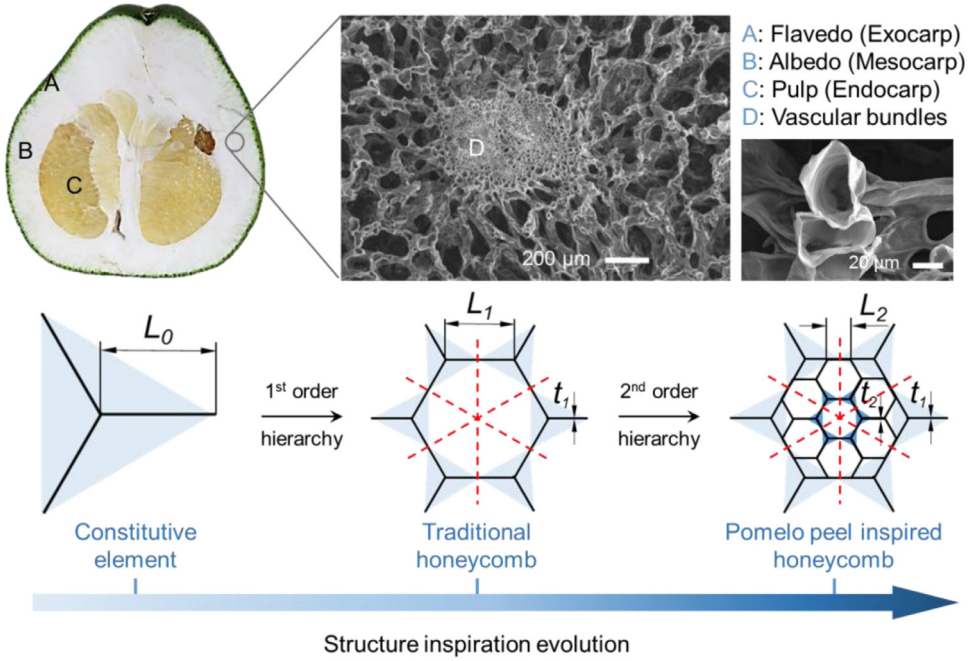

Fig. 1. Multi-scale diagrams and SEM photographs for depicting detailed microstructures of typical pomelo peel (A, B, C and D represent flavedo, albedo, pulp and vascular bundles, respectively), along with configurations and geometric parameters of pomelo peel inspired hierarchical honeycomb.

[20] and the arrangement of vascular bundles [17]) can not only help to understand the structural properties of pomelo peel, but provide insights in designing novel hierarchical structures with optimum energy absorption and crushing resistance performance for engineering applications. Actually, by combining X-ray tomographic imaging technique and digital volume correlation, the exploration on the internal mechanisms of structure-function relationship has revealed that the unique microstructure, i.e., vascular bundles connected by cells, plays an essential role in resistance performance of pomelo peel [21].

Compared to considerable amount of investigations on 1st order cellular materials [22–25], only few studies on hierarchical cellular materials are available due to the limitations in the fabrication approaches and experimental methods. Nevertheless, recent advances in fabricating technology-3D printing have augmented the field of hierarchical cellular materials research to help resolve the challenges and further understanding the fundamental mechanism of tailored properties [5,26–30]. In addition, it has been widely acknowledged that computational investigations via numerical analysis validated by robust experimental are crucial methodologies for exploration of advanced materials and novel structures in a computation efficient and cost effective manner [31,32]. Consequently, mechanical analysis and characterization of complex hierarchical cellular materials can be pursued by an integrated method combining theoretical, numerical and experimental approach nowadays, like the mechanical analysis of a vertex based hierarchical honeycomb [33,34] and other two-dimensional (2D) hierarchical honeycombs [35,36], indicating that improved mechanical properties can be achieved by applying structural hierarchy. It is also reported that proper arranged inclusions can help to artificially design the deformation process and mechanical properties of honeycomb structures [37,38].

In the present study, a focused investigation on the crushing resistance and energy absorption performance of a novel pomelo peel inspired hierarchical (two orders of hierarchy) honeycomb (shown in Fig. 1) under both out-of-plane and in-plane crushing is analyzed systematically via theoretical and finite element (FE) computational method. In Section 2, the validated experimental setting together with detailed finite element model for the pomelo peel inspired honeycomb is depicted. Section 3 presents the validation of FE model, critical crushing resistance criteria and representative results of pomelo peel inspired honeycomb under out-of-plane and in-plane crushing, underlying the mechanisms between optimum mechanical properties and specific structure. Finally, theoretical analysis for the equivalent plateau stress, parametric studies on the equivalent thickness (a significant parameter to describe the specific configuration, defined as t_2 / t_1, where t_1 and t_2 respectively represent the cell wall thickness of exterior honeycomb and interior honeycomb as shown in Fig. 1) and structural hierarchy are extensively performed to enhance the understanding of the clear correlation of structure and mechanical properties in Section 4.

2. Methods

2.1. Experimental setups

As shown in Fig. 2, the uniaxial compression experiments with a loading rate of 5 mm/min were performed on traditional honeycombs and pomelo peel inspired honeycombs made of aluminum alloy AA3003 H18 using INSTRON 8801 test machine with computer control

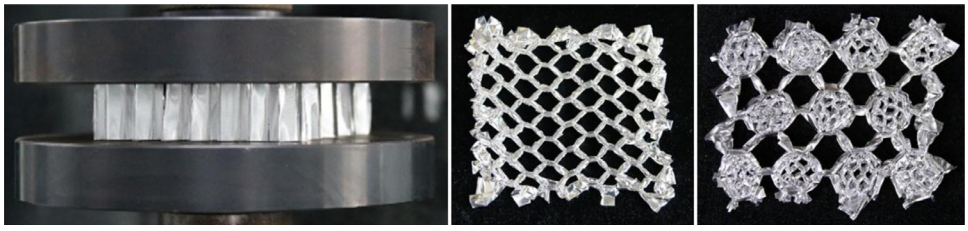

Fig. 2. Compressive test and representative deformation mode of traditional honeycomb and pomelo peel inspired honeycomb, where desired progressive folding pattern was observed in the tests.

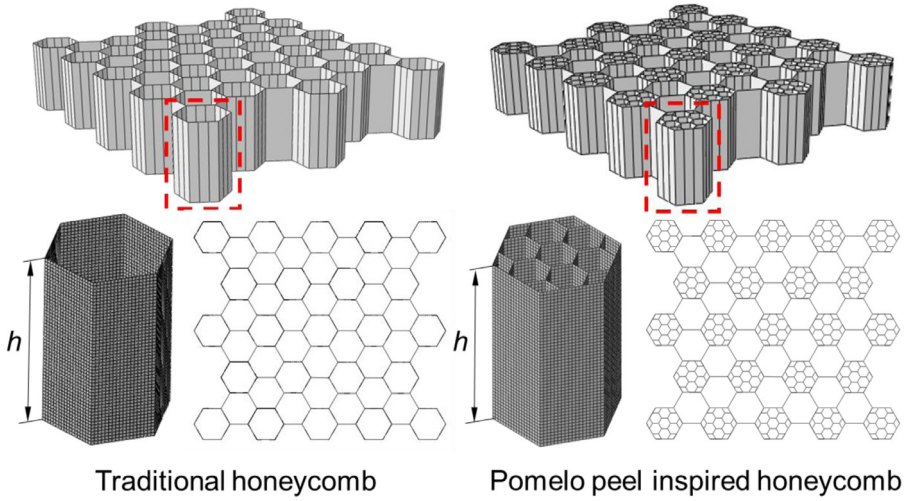

Fig. 3. Finite element models from different views for traditional honeycomb and pomelo peel inspired honeycomb.

and data acquisition system to obtain the load-displacement curves of the specimens. The traditional honeycomb used in our study was commercially available aluminum honeycomb core which could be cut into desired configurations with scissors. In view of pomelo peel inspired honeycomb consisting of two parts (exterior and interior honeycombs), we cut the interior honeycomb into separate small parts and inserted them into different cells of exterior honeycomb accordingly to fabricate the pomelo peel inspired honeycomb. The mechanical properties of honeycombs specimens with a thickness of $t_{1,\ 2} = 0.05$ mm, side length of $L_1 = 6$ mm, $L_2 = 2$ mm and height of $h = 20$ mm were investigated and three repeated tests were conducted.

2.2. Finite element model

The finite element code ABAQUS/EXPLICIT was employed to analyze the crushing properties of pomelo peel inspired honeycomb under both out-of-plane and in-plane dynamic loading. The finite element models with different hierarchical orders and corresponding dimensions are presented in Fig. 3, where the height (h) was set to be 20 mm, while the radius of inscribed circle for unit hexagonal cell in traditional and pomelo peel inspired honeycomb were set as 6 mm and 2 mm, respectively. The cell walls of the honeycombs in this study were modelled with shell elements (type S4R) and a convergence test with four different mesh sizes (0.2 mm, 0.4 mm, 0.6 mm and 0.8 mm) was carried out to obtain the computational confidence. In addition, double thickness was set accordingly in finite element models due to the specific manufacturing process of aluminum honeycomb. However, we considered cell walls with uniform thickness in following sections to avoid confusing and simplify the problem. In view of the balance between accuracy and computational cost, a mesh size of 0.4 mm was applied in the present study. Thus, the finite element models of traditional and pomelo peel inspired honeycomb totally consisted of 167,000 and 332,600 shell elements, respectively. General contact with a friction coefficient of 0.15 was defined and a rigid plane with a constant velocity of 15 m/s was applied for crushing the honeycombs dynamically. The free boundary condition was adopted on the free sides of finite element models. The base material of honeycomb is aluminum alloy AA6060 T4 with Young's modulus $E = 68.2$ GPa, yield stress of $\sigma_y = 80$ MPa, ultimate stress of $\sigma_u = 173$ MPa, Poisson's ratio of $\nu = 0.33$, power law exponent of $n = 0.23$ and density of $\rho = 2{,}700$ kg/m^3 [39]. When taking strain hardening effects into account, the elastic-perfectly plastic material assumption with a flow stress of $\sigma_0 = 106.1$ MPa calculated through σ_y, σ_u and n was employed for constitutive model in finite element analysis [40]. Considering the fact that aluminum alloys are strain rate insensitive, the influence of strain rate on material properties of honeycomb is trivial and thus neglected in the present study [34].

3. Results

3.1. Validation of FE model

In the present study, the finite element model was validated in accordance with the experimental data of both traditional honeycomb and pomelo peel inspired honeycomb, which may lay a solid foundation for the following parametric study. In addition, two critical principles are taken into consideration to guarantee the quasi-static numerical analysis in validation: (1) the total kinetic energy can be neglected when compared to the total internal energy during the crushing process; and (2) the load-displacement response is independent on the loading rate [41]. As illustrated in Fig. 4, it is obvious that numerical results suggest a good agreement with the experimental data for both traditional honeycomb and pomelo peel inspired honeycomb.

Apparently, the load-displacement curves can be divided into three typical stages, including elastic stage, plateau stage and densification stage, which is consistent with mechanical performance of other traditional honeycombs in previous literatures [[42–44]. Therefore, it is demonstrated that current FE modeling is reliable to describe the mechanical properties of pomelo peel inspired honeycomb.

3.2. Typical result

3.2.1. Crushing resistance criteria

To comprehensively understand the crushing properties and energy absorption performance of pomelo peel inspired honeycomb, crushing resistance criteria, containing specific energy absorption (*SEA*), crushing force efficiency (*CFE*) and equivalent plateau stress, are defined on the basis of load-displacement curve.

Specific energy absorption (*SEA*) serves as an essential criterion to assess the structural energy absorption per unit mass, which can be expressed as

$$SEA = \frac{EA}{m}, \tag{1}$$

where Energy absorption (*EA*) capacity and m are the total dissipated energy during the crushing process and mass of the structure, respectively. *EA*, which is defined in Eq. (2), has a direct correlation with the instantaneous crushing force $F(x)$ and the effective crushing deformation d (the length of the plateau stage), thus d is specified as 12 mm for out-of-plane crushing and 67 mm for in-plane crushing in the present

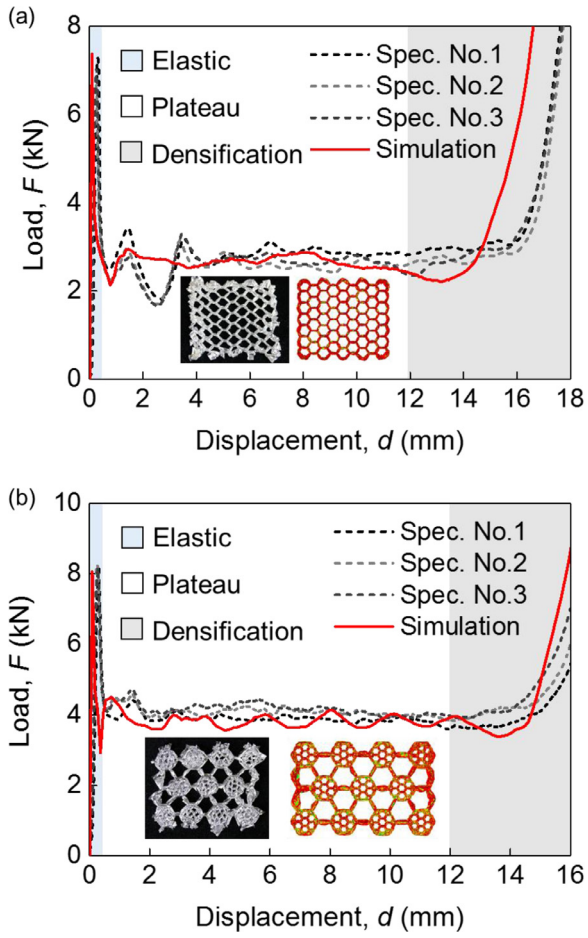

Fig. 4. Validation of finite element model by comparing load-displacement curves with experiments and computation results: (a) traditional honeycomb; (b) pomelo peel inspired honeycomb. Note that blue, white and grey areas represent for "Elastic Stage", "Plateau Stage" and "Densification Stage", respectively.

study for a fair comparison during parametric analysis.

$$EA = \int_0^d F(x)dx \tag{2}$$

It is well established that crushing force efficiency (*CFE*) is a critical criterion of crushing resistance assessment, especially for occupant protection in vehicle crash accidents [45] and it can be defined as

$$CFE = \frac{MCF}{PCF}, \tag{3}$$

where peak crushing force (*PCF*) can be directly obtained from the load-displacement curve and mean crushing force (*MCF*) represents the average force during the crushing process, which is expressed as

$$MCF = \frac{1}{d}\int_0^d F(x)dx = \frac{EA}{d}. \tag{4}$$

Furthermore, a non-dimensional equivalent plateau stress-$EA/(d\cdot\sigma_0\cdot A_e)$ is adopted to evaluate the crushing resistance of pomelo peel inspired honeycomb quantitatively, where σ_0 is the flowing stress of cell wall material mentioned before and A_e is defined as the authentic area of honeycombs (top view), effectively taking the material dosage into account.

3.2.2. Out-of-plane crushing computation

A representative load-displacement curve together with the illustration of energy absorption capacity of the pomelo peel inspired honeycomb under out-of-plane crushing is presented in Fig. 5, similar to the results of traditional honeycomb. Namely, a sharp load appears at the initial stage of crushing, then it falls rapidly and fluctuates around a certain value, and finally enters a continuous increasing stage. It is also demonstrated that the pomelo peel inspired honeycomb has a desirable regular progressive folding deformation mode, which can be defined as "hexagonal mode" from the top view of the structure. Nevertheless, the deformation mode may switch to an approximate circle (defined as "coin mode") as the increase of equivalent thickness, which will be carefully discussed in Section 4.2.

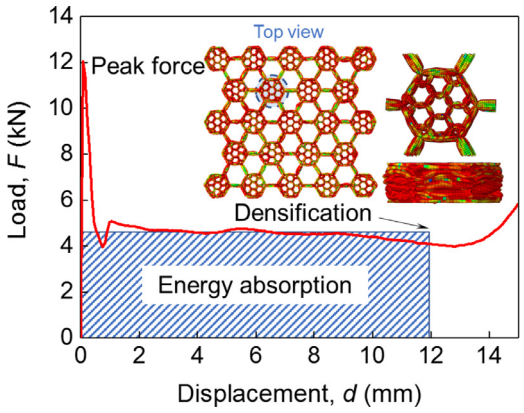

Fig. 5. Representative load-displacement curve and corresponding deformation mode of pomelo peel inspired honeycomb under out-of-plane crushing. "Three-stage" characteristic similar to traditional honeycomb and obvious localized plastic deformation in intersection among different panels are observed in numerical analysis.

3.2.3. In-plane crushing computation

As Fig. 6 shows, it is surprising that some interesting results are observed in pomelo peel inspired honeycomb under in-plane crushing, which is intimately linked to the equivalent thickness as well.

Actually, three typical localization bands of traditional honeycomb have already been reported and analyzed considering different loading rates based on numerical simulations in previous literature, consisting of "X" mode, "V" mode as well as "I" mode [46]. When it comes to the in-plane crushing of pomelo peel inspired honeycomb in the present study, a transitional mode: i.e. "V" mode can be obtained when $t_2/t_1 \leq 1$ (Fig. 6(a)), followed by a densification process. The initial localization occurs in a short time when the displacement is rather small and a "V" shaped band is developed close to the crushing plane. As the crushing proceeds, it appears that more layer of cells crush along with the propagation of "V" shaped band until the pomelo peel inspired honeycomb is fully crushed during the densification stage. Therefore, a simplified three-stage-model containing elastic, plateau and densification stages can be adopted for analyzing the mechanical properties of pomelo peel inspired honeycomb in this case.

However, a completely different result is observed in the case of $t_2/t_1 > 1$ (Fig. 6(b)), where "I" shaped band is found at the loading edge due to the restriction of lateral movement of the structure during crushing process. In addition, it is interesting to find a re-compression phenomenon after the exterior part of pomelo peel inspired honeycomb is totally crushed, which marks a 2nd energy absorption process. Hence, a modified model combined simplified three-stage-model with step load corresponding to each cell raw of the structure is constructed for describing the distinct crushing performance of pomelo peel inspired honeycomb in the case of $t_2/t_1 > 1$.

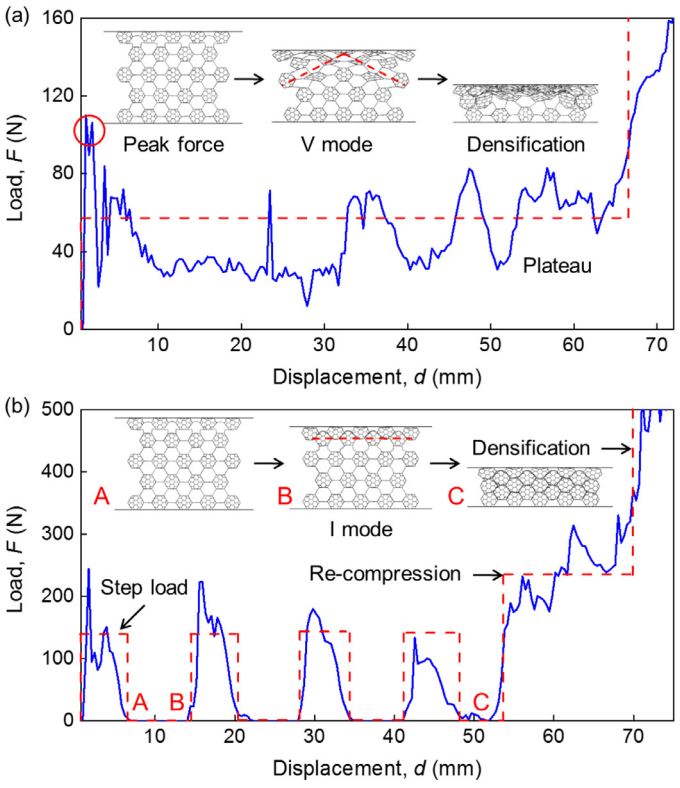

Fig. 6. Representative load-displacement curve together with corresponding deformation modes of pomelo peel inspired honeycomb under in-plane crushing: (a) $t_2/t_1 \le 1$; (b) $t_2/t_1 > 1$. Note that red dash lines represent idealized models demonstrating the typical characteristics of pomelo peel inspired honeycombs with different equivalent thickness.

4. Discussion

4.1. Theoretical model

4.1.1. Out-of-plane crushing

Constitutive elements with different central angles and edges including corner element, angle element with symmetric plane as well as angle element without symmetric plane are considered for developing the theoretical model of *MCF* for the pomelo peel inspired honeycomb under out-of-plane crushing. It is well noted that two assumptions of progressive thin-walled structures are adopted to simplify the problem, i.e. the rigid-perfectly plastic material and constant local buckling wave-length assumptions. In fact, previous literatures have investigated the crushing properties of different constitutive elements with different panel numbers (e.g. $N = 2, 3, 4$) and central angles (acute, right or obtuse angle) [47–49]. Based on their studies, the complex structure of pomelo peel inspired honeycomb can be divided into four different constitutive elements (type I, II, III, IV), which is shown in Fig. 7 and Table 1, making it accessible to a relatively simplified theoretical model for analyzing the crushing resistance of pomelo peel inspired honeycomb by summing up the contribution of every single element. In addition, the changes in geometric parameters of these constitutive elements, including the side length (B_1, B_2, B_3, $B_{4.1}$, $B_{4.2}$), wall thickness (t_1, t_2) and central angles (α, θ, γ, β), play an essential role in the energy dissipation process.

Table 1
Summary on detailed parameters of different element types for pomelo peel inspired honeycomb.

Element type	Geometric parameters	Number
Type I	t_1, $\alpha = 120^o$, $B_1 = \frac{1}{6}L_1$	$N_I = 38$
Type II	t_2, $\theta = 120^o$, $B_2 = \frac{1}{6}L_1$	$N_{II} = 276$
Type III	t_1, t_2, $\gamma = 60^o$, $B_3 = \frac{1}{6}L_1$	$N_{III} = 276$
Type IV	t_1, $\beta = 120^o$, $B_{4.1} = \frac{1}{6}L_1$, $B_{4.2} = \frac{1}{2}L_1$	$N_{IV} = 100$

The energy dissipation during a crushing process of pomelo peel inspired honeycomb mainly contains two parts, i.e. membrane energy and bending energy. Firstly, we can obtain the membrane energy of four different constitutive elements in two continuous folding wavelength since energy dissipation is different for the angle element without symmetric plane in two consecutive folds, which can be calculated as follows [41,50].

Type I (corner element):

$$W_{\text{membraneI}} = \frac{4M_1H^2}{t_1}\frac{\tan(\alpha/2)}{0.082(B_1/t_1)^{0.6}(\tan(\alpha/2) + 0.06/\tan(\alpha/2))}. \tag{5}$$

Type II (angle element with symmetric plane):

$$W_{\text{membraneII}} = \frac{4M_2H^2}{t_2}\frac{(20/1.2)^{0.6}(4\tan(\theta/4) + 2\sin(\theta/2) + 3\sin(\theta))}{(B_2/t_2)^{0.6}}. \tag{6}$$

Type III (angle element without symmetric plane):

$$W_{\text{membraneIII}} = \frac{4M_2H^2(20/1.2)^{0.6}}{t_2(B_3/t_2)^{0.6}}S_2 + \frac{4M_1H^2(20/1.2)^{0.6}}{t_1(B_3/t_1)^{0.6}}S_1, \tag{7}$$

where S_1 and S_2 can be expressed as

$$S_1 = \sin(\gamma/2 - 30^o) + 2\tan(\gamma/4 - 15^o) + 2\sin\gamma \tag{8}$$

and

$$S_2 = 2\tan(\gamma/4 + 15^o) + \sin(\gamma/2 + 30^o) + \sin\gamma. \tag{9}$$

Type IV (angle element with symmetric plane):

$$W_{\text{membraneIV}} = \frac{4M_1H^2(20/1.2)^{0.6}}{t_1}(G_1 + G_2), \tag{10}$$

where G_1 and G_2 can be expressed as

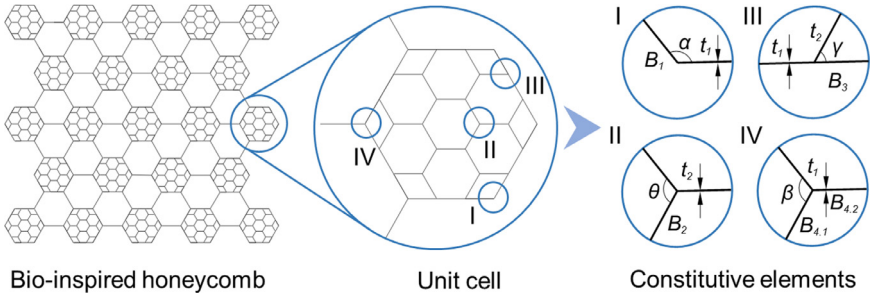

Fig. 7. Schematics of constitutive elements of pomelo peel inspired honeycomb. Different constitutive elements with distinct geometric dimensions are considered, consisting of corner element, angle element with symmetric plane, angle element without symmetric plane.

$$G_1 = \frac{4\tan(\beta/4) + 2\sin(\beta/2) + 2\sin(\beta)}{(B_{4.1}/t_1)^{0.6}} \tag{11}$$

and

$$G_2 = \frac{\sin(\beta)}{(B_{4.2}/t_1)^{0.6}}. \tag{12}$$

$M_{1,2}$ (shown in Eq. (13)) and H are the fully plastic bending moment of the flanges and half folding wave-length, respectively.

$$M_{1,2} = \frac{1}{4}\sigma_0 {t_{1,2}}^2, \tag{13}$$

where σ_0 is the flow stress introduced by Santosa and Wierzbicki et al. to calculate the energy equivalent flow stress of thin-walled material with power law hardening. It can be calculated as [40]

$$\sigma_0 = \sqrt{\frac{\sigma_y \sigma_u}{1+n}}. \tag{14}$$

As a result, when taking the number of different constitutive elements into account, the total energy dissipated by the membrane deformation in two continuous folding wave-length is achieved by

$$W_{\text{membrane}} = N_{\text{I}} W_{\text{membraneI}} + N_{\text{II}} W_{\text{membraneII}} + N_{\text{III}} W_{\text{membraneIII}} + N_{\text{IV}} W_{\text{membraneIV}}. \tag{15}$$

Afterwards, we can obtain the bending energy in two continuous folding wave-length through calculating the total energy dissipated at all the stationary hinge lines and it can be expressed as

$$W_{\text{bending}} = 2 \times 2\pi (M_2 L_{c2} + M_1 L_{c1}), \tag{16}$$

where $L_{c1} = 188L_1$ and $L_{c2} = 184L_1$ represent the total length of all flanges of exterior and interior part in pomelo peel inspired honeycomb, separately.

Consequently, the energy equilibrium of the pomelo peel inspired honeycomb is

$$MCF_a \times 4H \times \kappa = W_{\text{membrane}} + W_{\text{bending}}, \tag{17}$$

where κ is the coefficient of effective crushing distance. It has been reported that the effective crushing distance of three-panel angle element was smaller than that of square tube since the additional panel could reduce the available crushing distance, which is set to 0.7 in the present study [50]. Hence, we can acquire the half folding wave-length (H) through the stationary condition (showed in Eq. (18)) and substituting it into the energy equilibrium (Eq. (17)) to figure out the analytical result of *MCF*.

$$\partial MCF_a / \partial H = 0. \tag{18}$$

Given the fact that the inertia effects of dynamic cannot be neglected, a dynamic enhancement factor η is introduced to revise the theoretical model of pomelo peel inspired honeycomb. In view of the difference of constitutive elements discussed in present study, the dynamic enhancement factor was set to 1.2 in accordance with the work on three-panel angle elements [50]. Eventually, the theoretical model of *MCF* for pomelo peel inspired honeycomb can be given by

$$MCF_a = \frac{2\eta {L_1}^{0.2}\sigma_0}{\kappa}(A t_1^{1.6} + B t_2^{1.6})^{1/2}(C t_2^2 + D t_1^2)^{1/2}, \tag{19}$$

where $A = 4691.93$, $B = 10416.93$, $C = 144.51$, D=147.66.

Obviously, the mean crushing force we obtain is proportional to t with an exponent of 1.8. Actually, it has been reported that the ratio of the energy contribution between bending deformation and membrane deformation is closely related to this exponent [51]. If the exponent is 2, we know that it is a bending-only deformation, while the exponent is 1 for a membrane-only deformation. Furthermore, the exponent will range from 1 to 2 when both bending and membrane deformation are included. It is worthwhile to mention that the exponent is identical for traditional honeycomb and pomelo peel inspired honeycomb owing to their similar configurations of hexagonal honeycomb. Nevertheless, since the constant coefficient B in Eq. (19) is considerably larger than three other coefficients (A, C, D), it is clear that t_2 serves as an essential role in greater resistance performance to buckling. Namely, this pomelo peel inspired structure did improve the resistance performance when compared to traditional one.

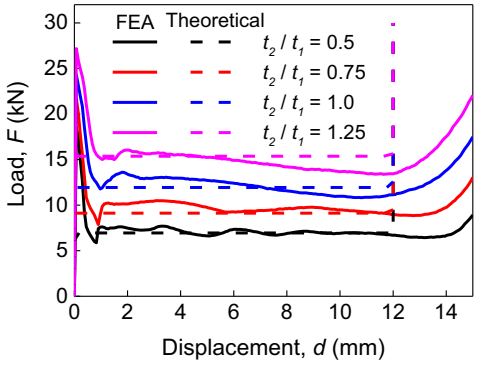

Fig. 8. Comparison for pomelo peel inspired honeycomb between theoretical model (dash line) and numerical analysis (solid line) under out-of-plane crushing.

It is obvious that the theoretical model is in good agreement with numerical analysis for pomelo peel inspired honeycomb with different equivalent thickness according to the comparison in Fig. 8.

4.1.2. In-plane crushing

Now that both the geometric configuration and collapse process of pomelo peel inspired honeycomb are associated with periodic characteristics under in-plane crushing (showed in Fig. 9(a) and (b)), a representative block can be obtained to analyze the crushing resistance of the entire structure. On the basis of previous studies that focused on the crushing resistance of traditional honeycomb and other novel configurations under in-plane crushing [52–54], theoretical models for pomelo peel inspired honeycomb are developed in consideration of the effect of equivalent thickness ($t_2/t_1 \le 1$ and $t_2/t_1 > 1$).

On one hand, it is demonstrated in Fig. 9(a) that the deformation mode of pomelo peel inspired honeycomb is quite similar to that of traditional honeycomb when $t_2/t_1 \le 1$ and the representative block of both interior and exterior part is presented here. Theoretical static plateau stress of traditional honeycomb has been investigated by Gibson and Ashby [55], which is described as

$$\sigma_s = \frac{2}{3}\sigma_0 \left(\frac{t}{L}\right)^2. \tag{20}$$

Nevertheless, the progressive localized densification under dynamic loading can be deemed as a structural impact, which is similar as the propagation of a plane plastic wave due to the hardening phenomenon with a locking strain in constitutive relationship of cellular material. Hence, a shock wave theory is applied to gain the theoretical dynamic plateau stress by using the following equation [46,54].

$$\sigma_d = \sigma_s + \frac{\rho^* v^2}{\varepsilon_d} \tag{21}$$

where v, ρ^* and ε_d denote the crushing velocity, density and locking strain of the honeycomb, respectively. It has been proven that hierarchical honeycomb has an earlier densification stage compared to the traditional honeycomb, thus an empirical expression is adopted to represent the locking strain of pomelo peel inspired honeycomb, i.e. $\varepsilon_d = 0.8(1 - \bar{\rho})$ [52]. And the density of traditional honeycomb is calculated as

$$\rho^* = \rho \times \frac{2}{\sqrt{3}} \times \frac{t_1}{L_1}. \tag{22}$$

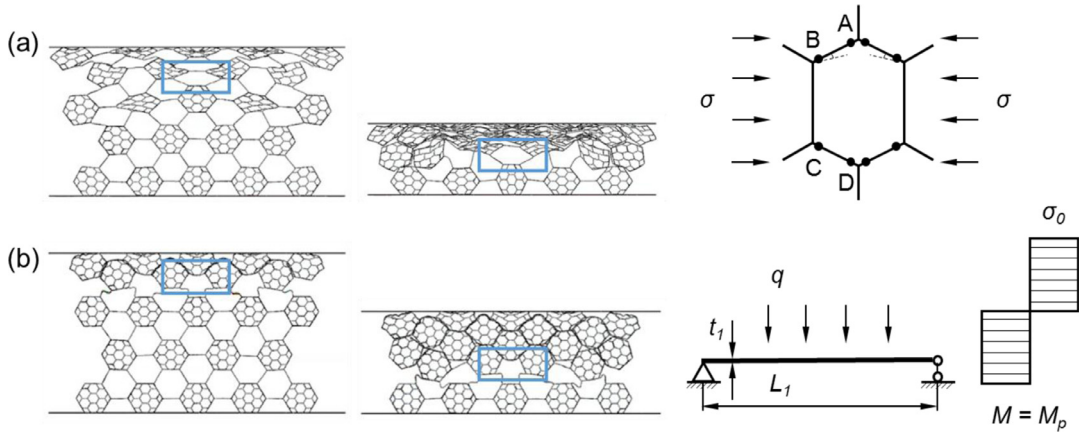

Fig. 9. A repeatable collapse process during the propagation of dynamic localized band and idealized representative blocks: (a) $t_2/t_1 \le 1$, "plastic hinges" are marked by A, B, C, D (black solid circles); (b) $t_2/t_1 > 1$.

Consequently, the integrated dynamic plateau stress can be estimated through combining the contribution of interior and exterior part of pomelo peel inspired honeycomb and then we can obtain the equivalent plateau stress through dividing the integrated plateau stress by the flow stress in the case of $t_2/t_1 \le 1$, which is given by

$$\sigma_e = \bar{\rho}_s \sigma_{di} + (1 - \bar{\rho}_s)\sigma_{de}. \tag{23}$$

where σ_{di}, σ_{de} and $\bar{\rho}_s$ represent dynamic plateau stress of interior, exterior part in pomelo peel inspired honeycomb and the relative density of structure, respectively. As is illustrated in Fig. 10(a), theoretical model for pomelo peel inspired honeycomb is in good agreement with the oscillating numerical result.

On the other hand, in view of the distinct deformation mode shown in Fig. 9(b), the conventional analytical method tends to be inappropriate for pomelo peel inspired honeycomb in the case of $t_2/t_1 > 1$. According to the numerical results, it is obvious that step load occurs whenever the top edge of exterior hexagonal cell is compressed during the in-plane crushing process, thus the energy dissipated by other deformation can be neglected in the step load stage and the simplified mode is also displayed in Fig. 9(b). Accordingly, the step load is easily given by making the maximum bending moment of the top edge (M) equals to the fully plastic bending moment (M_p), which can be expressed as

$$\frac{1}{8} q L_1^2 = \frac{1}{4}\sigma_0 (2t_1)^2. \tag{24}$$

where q denotes the load acting on unit length of top edge of exterior hexagonal cell and double thickness is adopted since two edges always overlap during the step load stage. It follows that the step stress is

$$q = \frac{8t_1^2}{L_1^2}\sigma_0. \tag{25}$$

It should be noted that the interior part of pomelo peel inspired honeycomb tends to have no deformation before the re-compression stage, therefore the analysis method of traditional honeycomb is appropriate for the re-compression stage of pomelo peel inspired honeycomb when $t_2/t_1 > 1$. Ultimately, the theoretical result combined step load and re-compression stage is consistent with that of the numerical analysis as presented in Fig. 10(b).

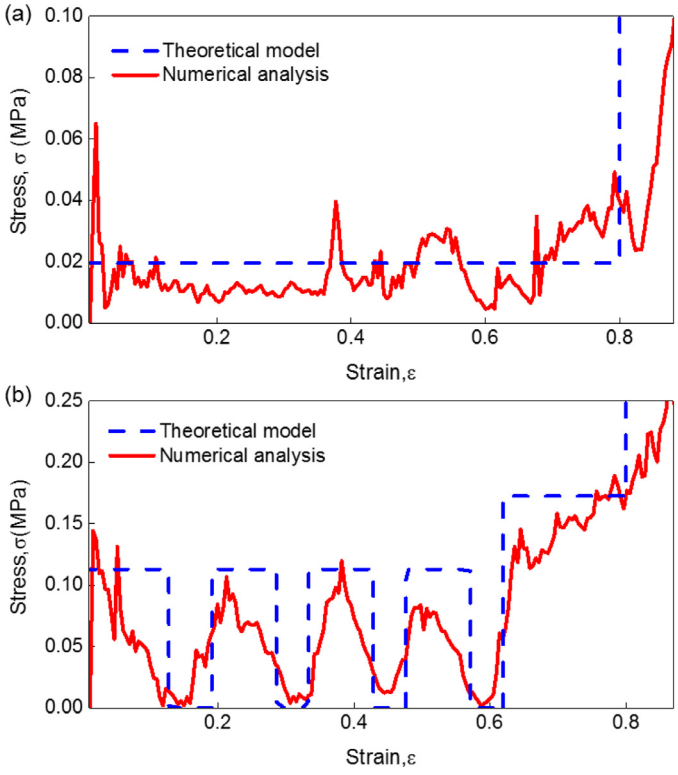

Fig. 10. Comparison for pomelo peel inspired honeycomb between theoretical model (dash line) and numerical analysis (solid line) under in-plane crushing: (a) $t_2/t_1 \le 1$; (b) $t_2/t_1 > 1$.

4.2. Effect of equivalent thickness

On the basis of previous analysis, it is demonstrated that the deformation mode of pomelo peel inspired honeycomb is governed by the equivalent thickness, meanwhile, the variation of equivalent thickness provides the additional flexibility in adjusting the material distribution of the whole structure. Therefore, a parametric study has been carried out to comprehensively understand the effect of equivalent thickness on the mechanical properties of pomelo peel inspired honeycomb under both out-of-plane and in-plane crushing. In addition, it is well acknowledged that the plateau stress and energy absorption performance of honeycomb structures are closely related to the relative density. The relative density of pomelo peel inspired honeycomb gives

$$\rho_r = \frac{\rho^*}{\rho_s} = \frac{V_m}{V} = \frac{(L_{c1}t_1 + L_{c2}t_2)h}{A \cdot h} = \frac{(L_{c1}t_1 + L_{c2}t_2)}{A}, \tag{26}$$

where ρ^* and ρ_s represent the density of the structure and the density of the solid counter-part, respectively. $L_{c1} = 188L_1$ and $L_{c2} = 184L_1$ represent the total length of all flanges of exterior and interior parts in pomelo peel inspired honeycomb. By adjusting the thickness values of exterior and interior honeycombs, various equivalent thickness values can be achieved for the same relative density. Fig. 11 displays the

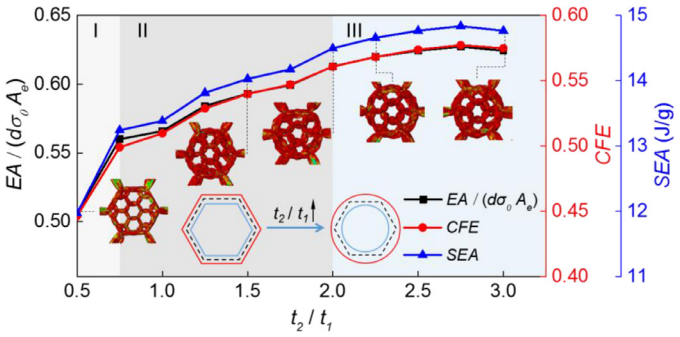

Fig. 11. The variation of crushing resistance criteria (equivalent plateau stress, *CFE, SEA*) and the deformation modes as an increase of equivalent thickness under out-of-plane crushing. Three typical modes (hexagonal mode, transitional mode and coin mode) are illustrated in accordance with different equivalent thickness levels, which is simplified by a schematic of representative block (black dash line represent the initial contour line, while the blue and red solid line represent inner and outer contour line after fully crushing, respectively).

numerical results of *CFE, SEA* and the equivalent plateau stress, together with the deformation modes of representative block in pomelo peel inspired honeycomb as an increase of equivalent thickness with identical relative density. Initially, there is a growing tendency of all the listed criteria with the increase of equivalent thickness, and later it tends to flatten, making it possible to regulate the crushing resistance and energy absorption performance of pomelo peel inspired honeycomb. Specifically, it is apparent that we can recover the traditional honeycomb at the limit when t_2 is close to zero. However, when t_1 is approaching zero, several separate traditional honeycombs will be obtained, which seems to be not attractive in this study.

Furthermore, three kinds of deformation modes (hexagonal mode, transitional mode and coin mode) of pomelo peel inspired honeycomb are observed in numerical analysis. It is seen that hexagonal mode with regular geometric profile appears in the pomelo peel inspired honeycomb with low equivalent thickness (about lower than 0.75), while the deformation mode turns into transitional mode with the increase of equivalent thickness and finally the coin mode is formed under rather high equivalent thickness (about higher than 2), also depicted by the simplified contour lines of representative block in Fig. 11. Actually, on account of growing circumferential stress under an increase of equivalent thickness, radial expansion of the exterior part constitutes the decisive factor for the transition of deformation modes for pomelo peel inspired honeycomb.

When it comes to the in-plane crushing of pomelo peel inspired honeycomb, two different cases ($t_2/t_1 \le 1$, $t_2/t_1 > 1$) with identical relative density are discussed in the parametric study.

As illustrated in Fig. 12, on one hand, *SEA* and the equivalent plateau stress generally increase with the equivalent thickness in the case

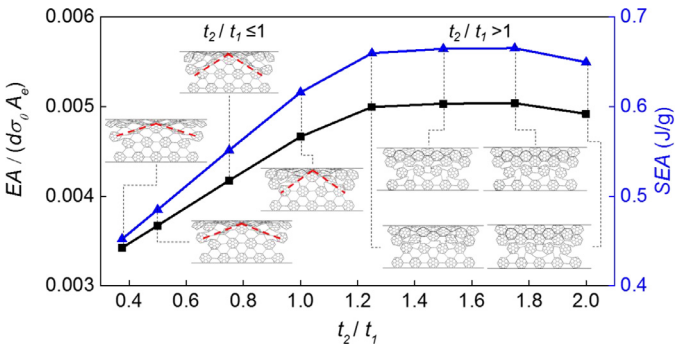

Fig. 12. The variation of crushing resistance criteria (equivalent plateau stress, *SEA*) and corresponding deformation modes as an increase of equivalent thickness under in-plane crushing.

of $t_2/t_1 \le 1$. Additionally, according to the deformation modes, the angles of "V" mode of the honeycombs are different since more hexagonal cells of pomelo peel inspired honeycomb deform in the preliminary crushing stage under a lower equivalent thickness. On the other hand, in the case of $t_2/t_1 > 1$, these two criteria both show a slowly changing trend as the equivalent thickness increases, and all the honeycombs reveal a consistent deformation mode, i.e. "I" mode, whereas interior part of pomelo peel inspired honeycomb with a higher equivalent thickness tends to be more neatly organized before recompression process. One possible explanation can be that the deformation of exterior part in the entire structure contributes less to the energy absorption and crushing resistance as the increase of equivalent thickness. Consequently, the influence of equivalent thickness not only reflects on the deformation modes but on the critical mechanism of energy absorption in pomelo peel inspired honeycomb.

4.3. Effect of structural hierarchy

Generally, the applications of hierarchical structures in engineering enable the increase of mechanical performance, thus it is quite essential to investigate the effect of structural hierarchy on crushing resistance and energy absorption performance of pomelo peel inspired honeycomb in the present study.

Due to the lack of commercially available aluminum honeycomb with nonstandard geometric parameters, it tends to be hard to carry out the experiments in order to compare the crushing resistance and energy performance of traditional and pomelo peel inspired honeycombs using a fair crashworthiness. However, this can be easily achieved by numerical analysis. Fig. 13 exhibits the comparison of *SEA* and equivalent plateau stress for traditional and pomelo peel inspired honeycomb with identical relative density for a fair comparison under both out-of-plane and in-plane crushing. It appears that *SEA* and equivalent plateau stress of pomelo peel inspired honeycomb are about 1.5 times than those of traditional honeycomb under out-of-plane crushing and approximate 2.5 times under in-plane crushing, demonstrating that structural hierarchy can substantially improve the crushing resistance and energy absorption property of the structure. It has been proven that both traditional and pomelo peel inspired honeycombs possess similar progressive folding deformation mode under out-of-plane crushing and "V" mode ($t_2/t_1 \le 1$ for pomelo peel inspired honeycomb) under in-plane crushing, while the additional interior hexagons in pomelo peel inspired honeycomb provide more corners and edges for localized plastic deformation and thus leading to outstanding energy absorption performance.

When compared to other typical engineering and natural materials as well as hierarchical structures, it is indicated that pomelo peel inspired honeycombs possess high energy absorption performance and high specific strength according to Ashby plot shown in Fig. 14, making it a potential engineering material for both vehicle structural designs and aerospace applications.

5. Concluding remarks

In this paper, the crushing resistance and energy absorption performance of pomelo peel inspired honeycomb was comprehensively investigated under out-of-plane and in-plane crushing analytically and numerically. Interesting deformation modes (desirable progressive folding with hexagonal/transitional/coin type under out-of-plane crushing and "V" /" I" type localized band with layer-by-layer crushing in the case of in-plane crushing) are observed thanks to variation of the equivalent thickness. On the basis of revealed deformation modes, theoretical models are constructed to derive the analytical results for evaluating the crushing resistance and energy absorption properties of pomelo-inspired honeycomb, which is well validated by the numerical analysis. It has been demonstrated that structural hierarchy plays a critical role in optimizing the crushing resistance and energy absorption

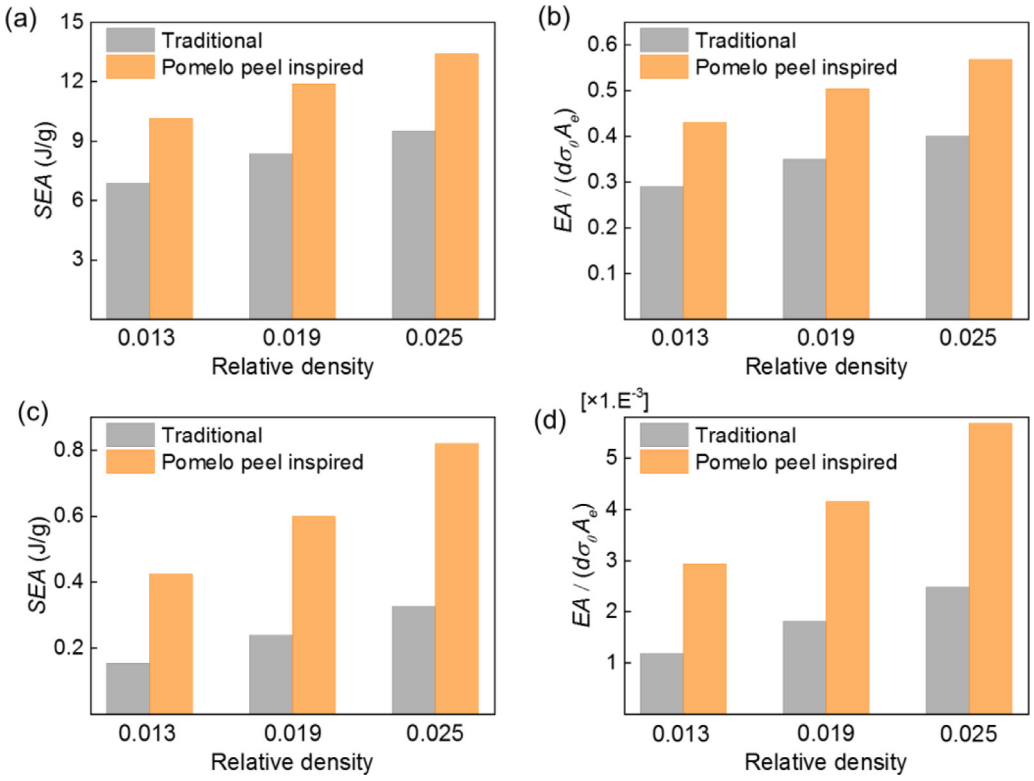

Fig. 13. The effect of structural hierarchy on *SEA* and equivalent plateau stress under (a) (b) out-of-plane and (c) (d) in-plane crushing. We use the identical relative density of traditional honeycomb and pomelo peel inspired honeycomb for a fair comparison. Generally, a distinct improvement is obtained via structural hierarchy, especially under in-plane crushing. Even if the absolute value of crushing resistance criteria is increasing with relative density, the ratio of these criteria between pomelo peel inspired honeycomb and traditional honeycomb keeps constant approximately.

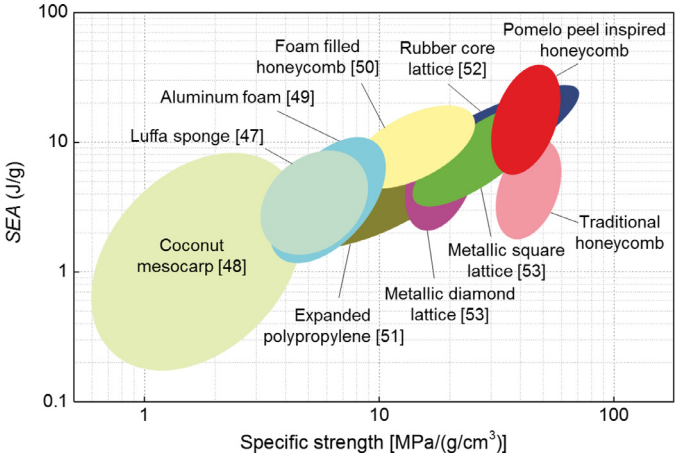

Fig. 14. Ashby plot illustrating the comparison of *SEA* and specific strength among pomelo peel inspired honeycomb and other typical materials [56–62].

capability. The *SEA* and equivalent plateau stress for hierarchical honeycomb can be up to 1.5 (out-of-plane crushing) and 2.5 times (in-plane crushing) than that of common honeycomb. Naturally, the understanding of its strain rate dependent behavior will be greatly enhanced if the fundamental deformation behavior is unraveled. A systematic study of the strain rate behavior of pomelo peel inspired honeycomb will be reported in the future. This work may offer insights in structural design and serve as a guiding step towards engineering application of hierarchical materials with superior mechanical performance.

Acknowledgement

This work is financially supported by Natural Science Foundation of China (Grant Nos. U1664250 and 11402012), Start-up funds of "The Recruitment Program of Global Experts" awardee and Fundamental Research Funds for the Central Universities, Beihang University.

Supplementary materials

Supplementary material associated with this article can be found, in the online version, at doi:10.1016/j.ijimpeng.2018.11.014.

References

[1] Berger JB, Wadley HNG, McMeeking RM. Mechanical metamaterials at the theoretical limit of isotropic elastic stiffness. Nature 2017;543:533–7.
[2] Grunenfelder LK, Suksangpanya N, Salinas C, Milliron G, Yaraghi N, Herrera S, Evans-Lutterodt K, Nutt SR, Zavattieri P, Kisailus D. Bio-inspired impact-resistant composites. Acta Biomaterialia 2014;10:3997–4008.
[3] Chintapalli RK, Breton S, Dastjerdi AK, Barthelat F. Strain rate hardening: A hidden but critical mechanism for biological composites? Acta Biomaterialia 2014;10:5064–73.
[4] Yu TX, Qiu X. Introduction to impact dynamics. Tsinghua University Press; 2018.
[5] Truby RL, Lewis JA. Printing soft matter in three dimensions. Nature 2016;540:371–8.
[6] Gao H. Application of fracture mechanics concepts to hierarchical biomechanics of bone and bone-like materials. Int J Fract 2006;138:101–37.
[7] Fratzl P, Weinkamer R. Nature's hierarchical materials. Progr Mater Sci 2007;52:1263–334.
[8] Wegst UGK, Bai H, Saiz E, Tomsia AP, Ritchie RO. Bioinspired structural materials. Nat Mat 2015;14:23–36.
[9] Zhao N, Wang Z, Cai C, Shen H, Liang F, Wang D, Wang C, Zhu T, Guo J, Wang Y, Liu X, Duan C, Wang H, Mao Y, Jia X, Dong H, Zhang X, Xu J. Bioinspired materials: from low to high dimensional structure. Adv Mater 2014;26:6994–7017.
[10] Wei X, Filleter T, Espinosa HD. Statistical shear lag model - Unraveling the size effect in hierarchical composites. Acta Biomaterialia 2015;18:206–12.
[11] Tan T, Rahbar N, Allameh SM, Kwofie S, Dissmore D, Ghavami K, Soboyejo WO. Mechanical properties of functionally graded hierarchical bamboo structures. Acta Biomaterialia 2011;7:3796–803.
[12] Huang W, Hongjamrassilp W, Jung J-Y, Hastings PA, Lubarda VA, McKittrick J. Structure and mechanical implications of the pectoral fin skeleton in the Longnose Skate (Chondrichthyes, Batoidea). Acta Biomaterialia 2017;51:393–407.
[13] Gross J, Timberg R, Graef M. Pigment and Ultrastructural Changes in the Developing Pummelo Citrus grandis 'Goliath'. Botanical Gazette 1983;144:401–6.
[14] Morton JF. Fruits of warm climates. In: Morton JF, editor. Distributed by Creative Resource Systems; 1987.
[15] Buehrig-Polaczek A, Fleck C, Speck T, Schueler P, Fischer SF, Caliaro M, Thielen M. Biomimetic cellular metals-using hierarchical structuring for energy absorption. Bioinspiration Biomim. 2016;11.

[16] Fischer SF, Thielen M, Loprang RR, Seidel R, Fleck C, Speck T, Buehrig-Polaczek A. Pummelos as concept generators for biomimetically inspired low weight structures with excellent damping properties. Adv Eng Mater 2010;12:B658–63.
[17] Thielen M, Schmitt CNZ, Eckert S, Speck T, Seidel R. Structure-function relationship of the foam-like pomelo peel (Citrus maxima)-an inspiration for the development of biomimetic damping materials with high energy dissipation. Bioinspiration Biomim 2013;8.
[18] Wang D, Zhang H, Guo J, Cheng B, Cao Y, Lu S, Zhao N, Xu J. Biomimetic gradient polymers with enhanced damping capacities. Macromol Rapid Commun 2016;37:655–61.
[19] Thielen M, Speck T, Seidel R. Impact behaviour of freeze-dried and fresh pomelo (Citrus maxima) peel: influence of the hydration state. R Soc Open Sci 2015;2.
[20] Thielen M, Speck T, Seidel R. Viscoelasticity and compaction behaviour of the foam-like pomelo (Citrus maxima) peel. J Mater Sci 2013;48:3469–78.
[21] Wang B, Pan B, Lubineau G. Morphological evolution and internal strain mapping of pomelo peel using X-ray computed tomography and digital volume correlation. Mater Des 2018;137:305–15.
[22] Honig A, Stronge WJ. In-plane dynamic crushing of honeycomb. Part II: application to impact. Int J Mech Sci 2002;44:1697–714.
[23] Chung J, Waas AM. Compressive response of circular cell polycarbonate honeycombs under inplane biaxial static and dynamic loading - Part II: simulations. Int J Impact Eng 2002;27:1015–47.
[24] Yamashita M, Gotoh M. Impact behavior of honeycomb structures with various cell specifications - numerical simulation and experiment. Int J Impact Eng 2005;32:618–30.
[25] Xu S, Beynon JH, Ruan D, Lu G. Experimental study of the out-of-plane dynamic compression of hexagonal honeycombs. Compos Struct 2012;94:2326–36.
[26] Kolesky DB, Truby RL, Gladman AS, Busbee TA, Homan KA, Lewis JA. 3D Bioprinting of Vascularized, Heterogeneous Cell-Laden Tissue Constructs. Adv Mater 2014;26:3124–30.
[27] Murphy SV, Atala A. 3D bioprinting of tissues and organs. Nat Biotechnol 2014;32:773–85.
[28] Compton BG, Lewis JA. 3D-Printing of Lightweight Cellular Composites. Adv Mater 2014;26:5930–5.
[29] Tumbleston JR, Shirvanyants D, Ermoshkin N, Janusziewicz R, Johnson AR, Kelly D, Chen K, Pinschmidt R, Rolland JP, Ermoshkin A, Samulski ET, DeSimone JM. Continuous liquid interface production of 3D objects. Science 2015;347:1349–52.
[30] Oftadeh R, Haghpanah B, Vella D, Boudaoud A, Vaziri A. Optimal fractal-like hierarchical honeycombs. Phys Rev Lett 2014;113.
[31] Moreno MD, Ma K, Schoenung J, Davila LP. An integrated approach for probing the structure and mechanical properties of diatoms: Toward engineered nanotemplates. Acta Biomaterialia 2015;25:313–24.
[32] Chen L, Du B, Zhang J, Zhou H, Li D, Fang D. Numerical study on the projectile impact resistance of multi-layer sandwich panels with cellular cores. Latin Am J Solids Struct 2016;13:2576–95.
[33] Oftadeh R, Haghpanah B, Papadopoulos J, Hamouda AMS, Nayeb-Hashemi H, Vaziri A. Mechanics of anisotropic hierarchical honeycombs. Int J Mech Sci 2014;81:126–36.
[34] Ajdari A, Jahromi BH, Papadopoulos J, Nayeb-Hashemi H, Vaziri A. Hierarchical honeycombs with tailorable properties. Int J Solids Struct 2012;49:1413–9.
[35] Fan HL, Jin FN, Fang DN. Mechanical properties of hierarchical cellular materials. Part I: Analysis. Compos Sci Technol 2008;68:3380–7.
[36] Chen Q, Pugno NM. In-plane elastic buckling of hierarchical honeycomb materials. Eur J Mech a-Solids 2012;34:120–9.
[37] Nakamoto H, Adachi T, Araki W. In-plane impact behavior of honeycomb structures randomly filled with rigid inclusions. Int J Impact Eng 2009;36:73–80.
[38] Nakamoto H, Adachi T, Araki W. In-plane impact behavior of honeycomb structures filled with linearly arranged inclusions. Int J Impact Eng 2009;36:1019–26.
[39] Sun G, Jiang H, Fang J, Li G, Li Q. Crashworthiness of vertex based hierarchical honeycombs in out-of-plane impact. Mater Des 2016;110:705–19.
[40] Santosa SP, Wierzbicki T, Hanssen AG, Langseth M. Experimental and numerical studies of foam-filled sections. Int J Impact Eng 2000;24:509–34.
[41] Zhang X, Zhang H. Energy absorption of multi-cell stub columns under axial compression. Thin-Walled Struct 2013;68:156–63.
[42] Zhang Y, Lu M, Wang CH, Sun G, Li G. Out-of-plane crashworthiness of bio-inspired self-similar regular hierarchical honeycombs. Compos Struct 2016;144:1–13.
[43] Zhang X, Zhang H, Wen Z. Experimental and numerical studies on the crush resistance of aluminum honeycombs with various cell configurations. Int J Impact Eng 2014;66:48–59.
[44] Ivanez I, Fernandez-Canadas LM, Sanchez-Saez S. Compressive deformation and energy-absorption capability of aluminium honeycomb core. Compos Struct 2017;174:123–33.
[45] Yin S, Li J, Liu B, Meng K, Huan Y, Nutt SR, Xu J. Honeytubes: Hollow lattice truss reinforced honeycombs for crushing protection. Compos Struct 2017;160:1147–54.
[46] Ruan D, Lu G, Wang B, Yu TX. In-plane dynamic crushing of honeycombs - a finite element study. Int J Impact Eng 2003;28:161–82.
[47] Zhang X, Zhang H. Theoretical and numerical investigation on the crush resistance of rhombic and kagome honeycombs. Compos Struct 2013;96:143–52.
[48] Zhang X, Huh H. Crushing analysis of polygonal columns and angle elements. Int J Impact Eng 2010;37:441–51.
[49] Kim HS. New extruded multi-cell aluminum profile for maximum crash energy absorption and weight efficiency. Thin-Walled Struct 2002;40:311–27.
[50] Zhang X, Zhang H. Numerical and theoretical studies on energy absorption of three-panel angle elements. Int J Impact Eng 2012;46:23–40.
[51] Lu G, Yu T. Energy absorption of structures and materials. Elsevier; 2003.
[52] Qiao J, Chen C. In-plane crushing of a hierarchical honeycomb. Int J Solids Struct 2016;85-86:57–66.
[53] Zhang D, Fei Q, Zhang P. In-plane dynamic crushing behavior and energy absorption of honeycombs with a novel type of multi-cells. Thin-Walled Struct 2017;117:199–210.
[54] Hu LL, Yu TX. Dynamic crushing strength of hexagonal honeycombs. Int J Impact Eng 2010;37:467–74.
[55] Gibson LJ, Ashby MF. Cellular Solids: structure and properties. Cambridge University Press; 1997.
[56] Shen J, Xie YM, Huang X, Zhou S, Ruan D. Mechanical properties of Luffa sponge. J Mech Behav Biomed Mater 2012;15:141–52.
[57] Xuan Truong N, Hou S, Liu T, Han X. A potential natural energy absorption material - Coconut mesocarp: Part A: Experimental investigations on mechanical properties. Int J Mech Sci 2016;115:564–73.
[58] Idris MI, Vodenitcharova T, Hoffman M. Mechanical behaviour and energy absorption of closed-cell aluminium foam panels in uniaxial compression. Mater Sci Eng a-Struct Mater Prop Microstruct Process 2009;517:37–45.
[59] Liu Q, Fu J, Wang J, Ma J, Chen H, Li Q, Hui D. Axial and lateral crushing responses of aluminum honeycombs filled with EPP foam. Compos Part B-Eng 2017;130:236–47.
[60] Avalle M, Belingardi G, Montanini R. Characterization of polymeric structural foams under compressive impact loading by means of energy-absorption diagram. Int J Impact Eng 2001;25:455–72.
[61] Yin S, Wu L, Ma L, Nutt S. Hybrid truss concepts for carbon fiber composite pyramidal lattice structures. Compos Part B-Eng 2012;43:1749–55.
[62] Queheillalt DT, Wadley HNG. Cellular metal lattices with hollow trusses. Acta Materialia 2005;53:303–13.